J Geod (2005)
DOI 10.1007/s00190-005-0459-9

ORIGINAL ARTICLE

O. Titov · P. Tregoning

Effect of post-seismic deformation on earth orientation parameter estimates from VLBI observations: a case study at Gilcreek, Alaska

Received: 22 September 2004 / Accepted: 18 April 2005 / Published online: 20 June 2005

Abstract Earth orientation parameters (EOPs) provide a link between the International Celestial Reference Frame (ICRF) and the International Terrestrial Reference Frame (ITRF). Natural geodynamic processes, such as earthquakes, can cause the motion of stations to become discontinuous and/or non-linear, thereby corrupting the EOP estimates if the sites are assumed to move linearly. The VLBI antenna at the Gilcreek Geophysical Observatory has undergone non-linear, post-seismic motion as a result of the $M_w = 7.9$ Denali earthquake in November 2002, yet some VLBI analysts have adopted co-seismic offsets and a linear velocity model to represent the motion of the site after the earthquake. Ignoring the effects of the Denali earthquake leads to error on the order of 300–600 μas for the EOP, while modelling the post-seismic motion of Gilcreek with a linear velocity generates errors of 20–50 μas. Only by modelling the site motion with a non-linear function is the same level of accuracy of EOP estimates maintained. The effect of post-seismic motion on EOP estimates derived from the International VLBI Service IVS-R1 and IVS-R4 networks are not the same, although changes in network geometries and equipment improvements have probably affected the estimates more significantly than the earthquake-induced deformation at Gilcreek.

Keywords Very long baseline interferometry (VLBI) · Post-seismic deformation · Earth orientation parameters (EOP) estimation · Terrestrial reference frame · Denali earthquake

O. Titov (✉)
Geoscience Australia,
GPO Box 378, Canberra, ACT 2601, Australia
Tel.: +61-2-62499064
Fax: +61-2-62499929
E-mail: oleg.titov@ga.gov.au

P. Tregoning
Research School of Earth Sciences,
The Australian National University,
Canberra, ACT 0200, Australia
E-mail: pault@rses.anu.edu.au

1 Introduction

The current internal precision of Earth orientation parameter (EOP) estimates from very long baseline interferometry (VLBI) data analysis of the International Earth Rotation Service (IERS) is on the order of ∼0.10–0.12 mas (Feissel-Vernier et al. 2004). However, Gambis (2004) showed that the accuracy in the combined IERS C04 EOP time series derived from satellite laser ranging (SLR), global positioning system (GPS) and VLBI techniques is at the level of 0.2–0.3 mas. Gambis (2004) suggested that the propagation of errors into the realization of the International Celestial Reference Frame (ICRF) and the International Terrestrial Reference Frame (ITRF) corrupt the daily EOP estimates and cause inconsistency between the internal precision and external accuracy. Haas (2004) analysed the methods of the operational EOP service by different groups, noting that the station positions are generally held fixed if daily EOPs are estimated from single 24 h VLBI sessions. Therefore, the a priori station coordinates must be known to be better than 5 mm to achieve the appropriate level of internal accuracy. However, geophysical processes such as co- and post-seismic earthquake deformation can affect the positions of VLBI observing stations by several orders of magnitude more than this amount.

The M_w=7.9 earthquake that occurred on the Alaska Peninsula on the 3 November 2002 ruptured the Denali, Susitna Glacier and Totschunda Faults (Eberhart-Phillips et al. 2003; Hreinsdóttir et al. 2003), and is located approximately 135 km south of Fairbanks (USA, 64°58′N, 147°30′W). The earthquake caused numerous landslides and measured surface offsets of up to 8.8 m (Eberhart-Phillips et al. 2003), with slip on the faults reaching 10 m (Hreinsdóttir et al. 2003). The GPS observing monument at Gilcreek Observatory was estimated to have moved by −52 mm, 25 mm and 23 mm, in North, East and Up directions, respectively (Eberhart-Phillips et al. 2003). Nothnagel (2003) provided an estimate of the co-seismic displacement (−59 mm North, 28 mm East, 14 mm Up) of Gilcreek using VLBI data from the first 6 months following the Denali earthquake. These values have been recommended

Table 1 Strategies used by different IVS Analysis Centers for the modeling of the Gilcreek VLBI site post-seismic motion

Solution	Strategy
USNO	Two sets of positions and common linear velocities are estimated [a]
BKG	Co-seismic offset and different values for post-seismic linear velocities (ITRF2000) [b]
IAA	Co-seismic offset and different values for post-seismic linear velocities (VTRF2003) [c]
MAO	Daily positions of the Gilcreek are unconstrained [d]
GSFC	Co-seismic effect and post-seismic exponential model[e]
GA	Co-seismic effect and post-seismic exponential model

USNO US Naval Observatory, *BKG* Bundesamt für Kartographie and Geodäsie, *IAA* Institute of Applied Astronomy, *MAO* Main Astronomical Observatory, *GSFC* Goddard Space Flight Center, *GA* Geoscience Australia
[a]from the IVS website
[b]V. Thorandt, personal communication
[c]E. Skurihina, personal communication
[d]S. Bolotin, personal communication
[e]D. MacMillan, personal communication

by the International VLBI Service (IVS) Analysis Coordinator to be used by VLBI analysts to model the kinematic motion of the site for the purpose of estimating EOPs.

The Gilcreek observatory actively participates in many VLBI observing programs. In this paper, we analyse several strategies used for approximating the post-seismic motion of Gilcreek and investigate the influence of the models on the daily EOP estimates. We compare our EOP time series (derived from various post-seismic models for Gilcreek site motion) to the IERS C04 EOP series, the basic reference of the IERS. We will show from an analysis of 18 months VLBI data after the earthquake that exponential models for the post-seismic period provide the best repeatability in all EOP components.

2 Different models of the Gilcreek site post-seismic motion

Different IVS Analysis Centers have implemented different procedures for modelling the post-seismic motion of Gilcreek (Table 1). Some adopt linear models for post-seismic velocities, in accordance with the ITRF2000 (Altamimi et al. 2002) or VTRF2003 (Nothnagel 2003) reference frame realizations. However, the post-seismic motion is not linear. Therefore, a more sophisticated approach may be required. Exponential models have been developed from VLBI data (Titov and Tregoning 2004; MacMillan and Cohen 2004) and GPS data (Prawirodirdjo and Bock 2004) to represent the site motion more accurately.

We have analysed the VLBI observations from programs NEOS-A (National Earth Orientation Service), IVS-R1 and IVS-R4 covering 2001.5–2004.4, and used our daily site coordinates to model the post-seismic motion. The observational programs contain 24 h sessions, with observations including 4–8 globally distributed VLBI sites. The VLBI site at Gilcreek participated in 74 daily observational sessions between July 2001 and the Denali earthquake, and 122 sessions after the earthquake until 5 May 2004. The dataset thus comprises 16 months before and 18 months after the earthquake. The analysis of the VLBI data has been performed using the OCCAM software (Titov et al. 2001), and the Geoscience Australia solution for radiosource positions aus2002 (Titov and Govind 2003) has been used to define the Celestial Reference Frame. All site coordinates were fixed to their VTRF2003 values (Nothnagel 2003) except Gilcreek, whose daily coordinates through the post-seismic period were estimated and are shown in Fig. 1a.

The observations of each daily session were processed individually using a Kalman filter to estimate nutation offsets, EOP, station positions of Gilcreek, VLBI clock offsets and rates, as well as tropospheric delays and horizontal tropospheric gradients. All parameters were considered to be deterministic except clock offsets and tropospheric delays that were modelled stochastically with a random walk model. In this paper, we present a new model (Model-A) for the post-seismic motion of Gilcreek, which is calculated from a longer observational period than Titov and Tregoning (2004) and MacMillan and Cohen (2004) Figure 1a also shows the approximate span of observations used in the estimation of the post-seismic Model-A and the linear VTRF model (Nothnagel 2003).

MacMillan and Cohen (2004) estimated Model-B using the SOLVE analysis program (Ma et al. 1990) to process the VLBI group delays. They estimated positions and velocities for all other VLBI stations as global parameters, and NNR- and NNT-constraints (No-Net-Rotation and No-Net-Translation of the daily site coordinate estimates in the TRF with respect to VTRF2003) were imposed on station positions and velocities.

Model-C (Prawirodirdjo and Bock 2004) was derived from daily site positions estimated from GPS data using the GAMIT software version 10.06 (King and Bock 2002). Daily EOPs were also estimated. GPS data were separated into 24 h segments to make the GPS time series for Gilcreek positions the same as the VLBI time series. Prawirodirdjo and Bock (2004) describe in more detail how their GPS analysis was performed.

The processes for generating daily site coordinates for Gilcreek were similar for each of the three models (Table 2) and, in general, the models are consistent at the level of several millimetres (Fig. 1b). Model-A implements a common post-seismic decay time for the North and East components.

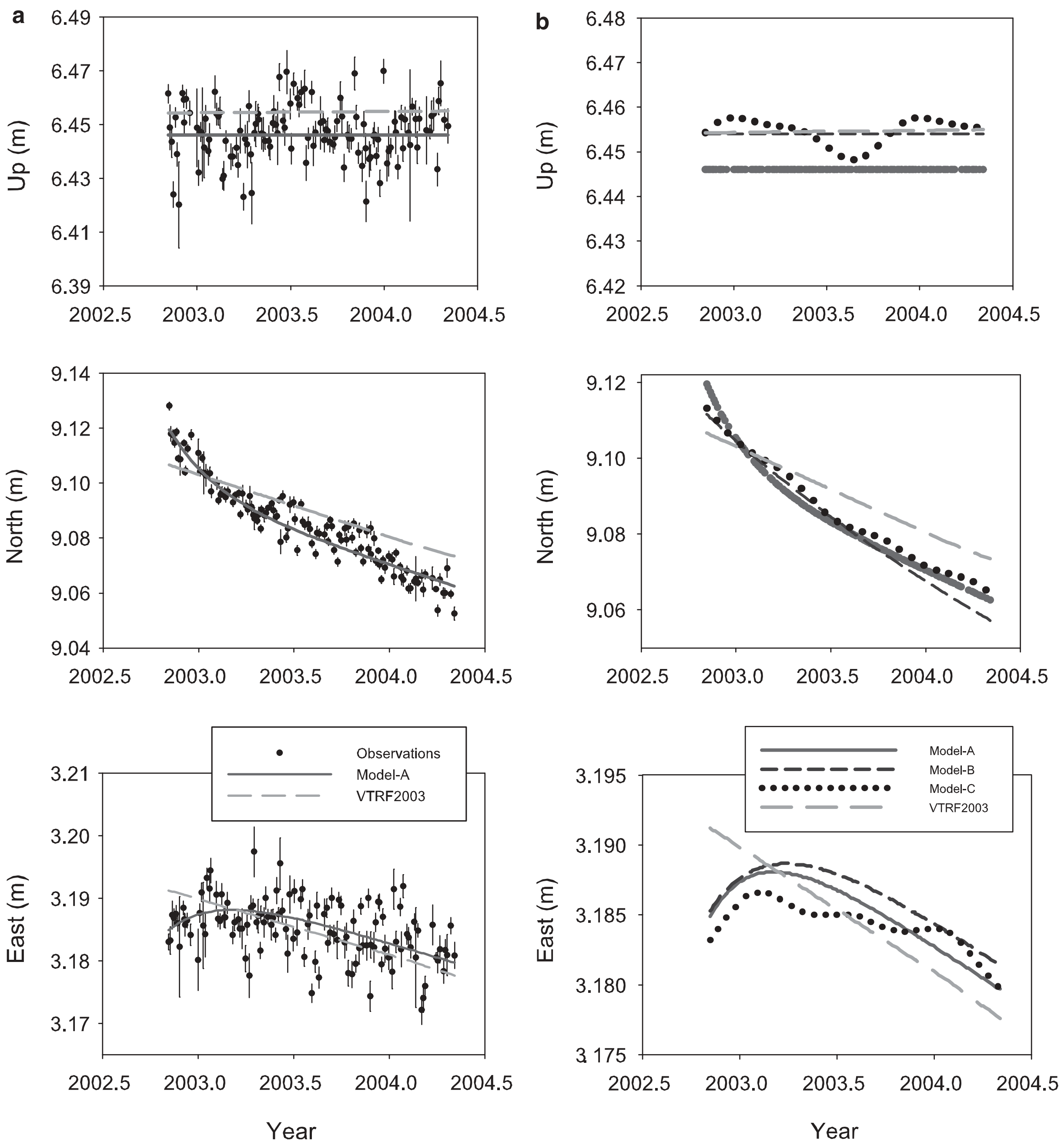

Fig. 1 **a** *Left column*: Daily coordinate estimates of the Gilcreek VLBI antenna for the first 18 months after the Denali earthquake. Site motion modelled as a linear velocity (*dashed line, green*) and exponential model (*solid line, red*) is shown for each component. **b** *Right column*: Site motion modelled as a linear velocity (*long dashed line, green*) and exponential models: Model-A (*solid line, red*), Model-B (*short dashed line, blue*) and Model-C (*dots, black*) as designated in Table 2

Table 2 Parameters of exponential models for three solutions: this paper (Model-A), MacMillan and Cohen (2004)(Model-B), Prawirodirdjo and Bock (2004)(Model-C)

Model	Time decay (year)			Co-seismic offset (mm)			Post-seismic amplitude (mm)			Seasonal terms
	Up	North	East	Up	North	East	Up	North	East	
Model-A	–	0.25	0.25	8	−47.8	22.6	0	−23.7	8.6	No
Model-B	–	1.18	0.32	16	−56	29	0	−29	10	No
Model-C	–	0.52	0.52	15.7	−54.8	21.1	0	−16.8	11.5	Yes

Model-B uses different values of the decay constant for the North and East components (1.18 and 0.32 years), although one might expect that the decay time would be equal for all components. Model-C also implements a common decay constant and, in addition, takes into account seasonal variations at the scale of up to several millimetres for all three components. In all three models, the vertical component does not appear to be affected by post-seismic relaxation, and thus a linear velocity is used.

3 Comparison of the EOP solutions

To analyse the effect of particular models on EOP estimates, the analysis strategy described in Sect. 2 was slightly modified. We fixed all station positions according to the VTRF2003 model, except Gilcreek, which was treated using two different post-seismic motion models throughout the post-seismic period. Below we discuss only the observing sessions that included Gilcreek.

Time series of EOP were estimated for the period 2001.5 to 2004.4 using four different analysis approaches. For Solution 1, the coordinates of Gilcreek were fixed and the effects of the Denali earthquake were ignored completely. The coordinates of Gilcreek were unconstrained both before and after the earthquake for Solution 2. Thus, Solution 2 is identical to the coordinate-solution in Sect. 2 throughout the post-seismic period. For Solution 3, the coordinates of Gilcreek were fixed and the co-seismic displacements and linear velocities of Nothnagel (2003) were adopted. In Solution 4, linear VTRF2003 velocities were used before the earthquake and the Gilcreek co-seismic offsets and exponential post-seismic motion of Model-A (Table 2) were applied. In addition, the post-seismic models of MacMillan and Cohen (2004) and Prawirodirdjo and Bock (2004) were used to generate Solutions 5 and 6, respectively. The resulting EOP estimates are shown in Fig. 2.

The co-seismic displacements used in Solution 4 differ from those of Nothnagel (2003) by only 6, −2 and 6 mm in North, East and Up, respectively. Both velocity models are nearly parallel 1.5 years after the earthquake, although there are offsets between the two models evident in each coordinate component that amount to position differences of −9 mm, 4 mm and −13 mm in North, East and Up, respectively at epoch 2004.4.

We calculated the differences between each of the time series and the IERS C04 EOP and IGS EOP time series separately for the pre- and post-seismic periods. The C04 EOP time series is a combination of results from different space-geodetic techniques (VLBI, GPS, SLR, DORIS) and represent the most accurate values for EOP. The IGS EOP time series is obtained from GPS data analysis only, completely independent of VLBI results, and provides an external evaluation of our VLBI solutions. The noise in the GPS-derived UT1-UTC series is significantly larger than that derived from VLBI observations and larger than the differences in the various VLBI EOP series mentioned above. Therefore, it cannot be used to assess the external precision of our UT1-UTC estimates and we restrict our EOP comparisons with the IGS series to only polar motion. The weighted root-mean-square (WRMS) differences of the EOPs are shown in Tables 3 and 4.

4 Discussion of the EOP estimates

The EOP time series from Solution 1 highlights the effect of an antenna displacement at a single site in the global VLBI network. The increase in WRMS differences is on the level of 300–600 µas (Table 1), indicating that the co-seismic movement of the Gilcreek VLBI antenna of about 62 mm must be accounted for. The time series resulting from Solution 2 shows that not using Gilcreek as a fiducial site causes a reduction of accuracy in the resulting EOP time series during the pre-seismic period. The WRMS differences increase by 40–80 µas and we found that unconstraining the coordinates of any of the fiducial sites resulted in a similar increase in WRMS. This highlights the fragility of the current VLBI networks for estimating EOPs. Whilst leaving the coordinates of Gilcreek unconstrained reduces the WRMS differences in the post-seismic period (compared to constraining them at incorrect values as in Solution 1), one still does not achieve the same level of accuracy as constraining the coordinates to the correct values (Solution 1, pre-seismic period).

Gilcreek is treated in the same manner in the pre-seismic period for Solutions 1 and Solutions 3 to 6. The WRMS differences of the post-seismic period of Solution 3 are 20–50 µas larger than during the pre-seismic period, indicating that the combination of co-seismic offsets and a post-seismic linear velocity degrades the accuracy of the site coordinates and hence the EOP estimates. Indeed, one generates more accurate post-seismic EOP estimates by treating Gilcreek as an unconstrained site (Solution 2) than by applying a linear post-seismic velocity model. The non-linear model for the post-seismic velocity in our Solution 4 yields EOP estimates with WRMS differences comparable to the pre-seismic period (Table 3).

The EOP estimates calculated using any of the exponential post-seismic models (Table 2, Solutions 4 to 6) are more precise than those using a linear model (Solution 3) and have a comparable precision to the pre-seismic period. Therefore, an exponential model is required for approximating the Gilcreek post-seismic motion in order to maintain the same level of EOP accuracy after the earthquake. We conclude that the linear model is inadequate for modelling the post-seismic motion and degrades the EOP time series.

The C04 EOP time series is combined from different space-geodetic techniques with a large contribution from VLBI observations. To check our conclusion above, we compared our solutions with the GPS EOP time series. The resulting WRMS differences in Table 4 are, in general, larger than in Table 3, confirming that our EOP solutions are closer to the C04 EOP than to the GPS EOP time series. However, it is clear that the exponential model for the post-seismic

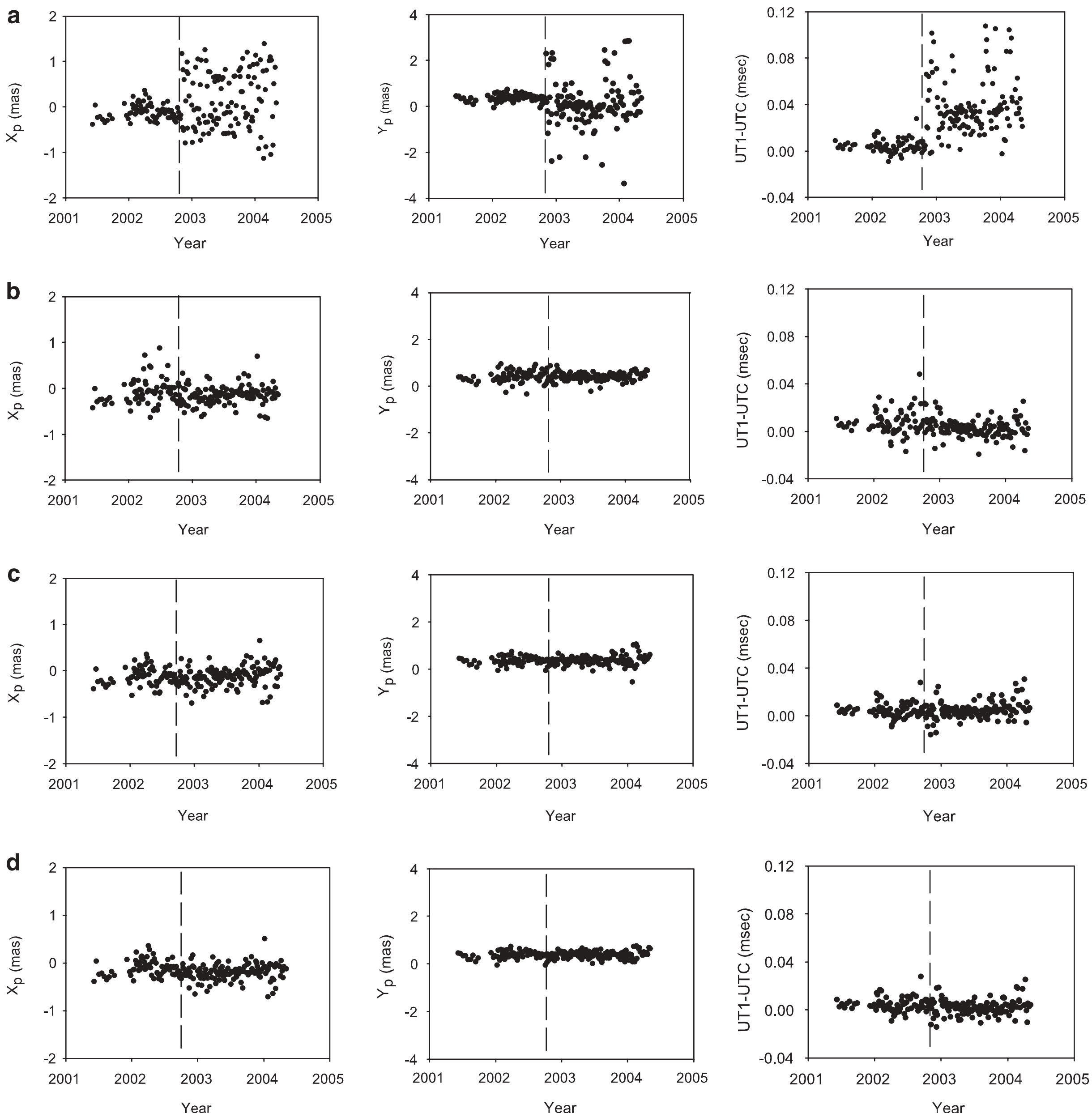

Fig. 2 Earth orientation parameter estimates spanning 2001.5 to 2004.4. **a** Solution 1 – Gilcreek station position is fixed to VTRF2003, **b** Solution 2 – Gilcreek station position is estimated, **c** Solution 3 – Gilcreek station position is modelled with a co-seismic displacement and a linear post-seismic motion, **d** Solution 4 – Gilcreek station position is modelled with a co-seismic displacement and an exponential post-seismic motion

Table 3 Weighted root-mean square differences of the six EOP solutions with respect to IERS C04 values for pre- and post-seismic periods. The Gilcreek station position was modelled: (1) no co- and post-seismic effects, (2) unconstrained Gilcreek, (3) linear model, (4) Model-A, (5) Model-B, (6) Model-C

Solution	Pre-seismic			Post-seismic		
	X-p (μas)	Y-p (μas)	UT1-UTC (μs)	X-p (μas)	Y-p (μas)	UT1-UTC (μs)
1	127	129	4.6	526	747	23.6
2	206	186	7.1	140	134	5.6
3	127	129	4.6	147	163	5.8
4	127	129	4.6	126	117	4.6
5	127	129	4.6	123	108	4.7
6	127	129	4.6	129	131	4.6

Table 4 The weighted root-mean square differences of the six EOP solutions with respect to EOP IGS values for pre- and post-seismic periods. The Gilcreek station position was modelled: (1) no co- and post-seismic effects, (2) unconstrained Gilcreek, (3) linear model, (4) Model-A, (5) Model-B, (6) Model-C

Solution	Pre-seismic		Post-seismic	
	X-p (μas)	Y-p (μas)	X-p (μas)	Y-p (μas)
1	172	139	552	760
2	221	178	160	150
3	172	139	173	180
4	172	139	138	145
5	172	139	140	123
6	172	139	149	147

motion still produces the best EOP estimates (Table 4). MacMillan and Cohen (2004) found from an analysis of the first 14 months of VLBI data after the earthquake that using a transient model to represent the post-seismic motion of Gilcreek reduced the WRMS from 130 μas to 115 μas and from 127 μas to 113 μas for X- and Y-pole components, respectively. Our analysis of a longer time span of data shows that this trend continues.

To ascertain whether other factors were affecting the accuracy of the EOP estimates, we considered the EOP estimates from the IVS-R1 and IVS-R4 networks separately. Both networks comprise a different set of VLBI stations. As such, the network configuration could cause additional inconsistencies in our statistics. As was shown by Feissel-Vernier et al. (2004) the EOP derived from the IVS-R1 and IVS-R4 networks over 2002.0–2003.8 are scattered at the level of 0.1 mas, based on EOP values estimated by MacMillan and Cohen (2004) using exponential motion Model B (MacMillan and Cohen 2004). In this paper, we evaluate the WRMS differences for the IVS-R1 and IVS-R4 networks, separately, using the approach of Solution 4. Gilcreek participated in 40 IVS-R1 sessions and 22 IVS-R4 sessions before the earthquake and 73 IVS-R1 sessions and 46 IVS-R4 sessions after the earthquake. Therefore, the resulting WRMS differences (shown in Table 5 for EOP C04) should be considered carefully because there are limited and unequal numbers of sessions before the earthquake.

For various reasons, some VLBI stations participated in both IVS-R1 and IVS-R4 networks (e.g. Wettzell, Gilcreek, Tigoconc, Kokee, Ny-Alesund), whereas others were scheduled for inclusion in just one of the two networks. In addition, the frequency of appearance for each individual VLBI site varies considerably. Hence, the investigation of the effect of the individual site coordinates on the resulting EOP time series is complicated by the uneven site distribution within the IVS-R1 and IVS-R4 networks.

The IVS-R4 network provides better estimates of the Y-pole component and UT1-UTC through the post-seismic period than the IVS-R1 network (Table 5). The differences between the WRMS differences of the two networks are less for the Y-pole component (about 20 μas) than for the X-pole component, and the WRMS differences for the Y-pole component are comparable to the values during the pre-seismic period. The WRMS differences for the X-pole component during the post-seismic period for the IVS-R4 network are about 80 μas larger than those for the IVS-R1 network. This inconsistency was not caused by the inadequate modelling of the Gilcreek post-seismic motion because the Gilcreek station participated in both networks and an inadequate model would corrupt the results from both networks.

Instead, it is more likely that changes in the set of sites included in each of the IVS-R1 and IVS-R4 sessions and the inclusion of a new site, Svetloe in IVS-R1 since March 2003 have led to changes in the performances of the two networks. The effects of these variations to network performances are beyond the scope of this paper; however, both network and equipment changes offer plausible explanations to apparent changes in EOP estimate precision and are currently the focus of an independent study.

5 Conclusion

A priori station coordinates have to be known to the level of about 5 mm to reach an appropriate precision of operational EOP estimates. It is not surprising that failing to account for the co-seismic displacement of a VLBI antenna (exceeding this level by an order of magnitude) causes a significant degradation of the estimates of EOPs. The effect of the 2002 Denali earthquake caused about 62 mm co-seismic displacement at Gilcreek, Alaska, and was followed by a period of non-linear post-seismic relaxation. Modelling the site motion during the post-seismic period with a linear velocity model actually produces less accurate EOP estimates than an analysis where the coordinates of the affected site are left completely unconstrained. This highlights the sensitivity of estimating EOP from sparse VLBI networks to small coordinate errors. It is only with the use of a non-linear post-seismic motion model for Gilcreek that the accuracy of the pre-seismic EOP estimates can be reproduced after the Denali earthquake.

Table 5 Weighted root-mean square differences of Solution 4 with respect to the IERS C04 values for pre- and post-seismic periods separately for the IVS-R1 and IVS-R4 networks

Network	Pre-seismic			Post-seismic		
	X-p (μas)	Y-p (μas)	UT1-UTC (μs)	X-p (μas)	Y-p (μas)	UT1-UTC (μs)
IVS-R1	119	149	5.6	89	132	5.4
IVS-R4	134	136	5.2	167	111	4.7

Acknowledgements We are thankful to Volkmar Thorandt (BKG), Elena Skurihina (IAA), Dan MacMillan (GSFC) and Sergei Bolotin (MAO) for comprehensive information about their Analysis Center procedures for treatment of the Gilcreek VLBI site over the post-seismic period. We thank Martine Feissel-Vernier (Paris Observatory), Axel Nothnagel (GIUB) and an anonymous reviewer for helpful comments that improved this manuscript.

References

Altamimi Z, Sillard P, Boucher C (2002) ITRF2000: A new release of the International Terrestrial Reference Frame for earth science applications. J Geophys Res 107(B10): 2114

Eberhart-Phillips D, Haeussler PJ, Freymueller JT, Frankel AD, Rubin CM, Craw P, Ratchkovski NA, Anderson G, Carver GA, Crone AJ, Dawson TE, Fletcher H, Hansen R, Harp EL, Harris RA, Hill DP, Hreinsdóttir S, Jibson RW, Jones LM, Kayen R, Keefer DK, Larsen CF, Moran SC, Personius SF, Plafker G, Sherrod B, Sieh K, Sitar N, Wallace WK (2003) The 2002 denali fault earthquake, Alaska: A large magnitude, slip-partitioned event. Science 300:1113–1118

Feissel-Vernier M, Ray J, Altamimi Z, Dehant V, de Viron O, (2004) VLBI and earth rotation: geophysical and geodetic challenges. In: Vandenberg N, Baver KD (eds) Proceedings IVS 2004 General meeting, NASA/CP-2004-212255, pp 22–31

Gambis D (2004) Monitoring earth orientation using space-geodetic techniques: state-of-art and prospective. J Geod 296–303

Haas R (2004) Analysis strategies and software for geodetic VLBI. In: Bachiller R, Colomer F, Desmurs JF, de Vicente P (eds) Proc the 7th European VLBI Network Symposium, Toledo, Spain, pp 297–301

Hreinsdóttir S, Freymueller JT, Fletcher HJ, Larsen CF, Bürgmann R (2003) Coseismic slip distribution of the 2002 M_w7.9 Denali fault earthquake, Alaska, determined from GPS measurements. Geophys Res Lett 30:1670. DOI 10.1029/2003GL017447

King R, Bock Y (2002) Documentation for the GAMIT GPS analysis software, release 10.06, Mass Inst of Technol, Cambridge

Ma C, Sauber JM, Bell LJ, Clark TA, Gordon D, Himwich WE, Ryan JW (1990) Measurement of horizontal motions in Alaska using very long baseline interferometry. J Geophys Res 95 (B13):21991

MacMillan D, Cohen S (2004) Postseismic Transient after the 2002 Denali Fault Earthquake from VLBI Measurements at Fairbanks, In: Vandenberg N, Baver KD (eds) Proc IVS 2004 General Meeting, NASA/CP-2004-212255, pp 491–495

Nothnagel A (2003) VTRF2003: a conventional VLBI terrestrial reference frame. In: Schwegmann W, Thorandt V (eds) Proceedings of the 16th working meeting on European VLBI for geodesy and astrometry, Leipzig, pp 195–205

Prawirodirdjo L, Bock Y (2004) Instantaneous global plate motion model from 12 years of continuous GPS observations. J Geophys Res 109:B08405. DOI 10.1029/2003JB002944

Titov O, Govind R (2003) Geoscience Australia IVS Analysis Center. In: Vandenberg N, Baver KD (eds) IVS 2002 Annual Report, NASA/TP-2003-211619, pp 225–227

Titov O, Tesmer V, Boehm J (2001) OCCAM 5.0 User Guide, AUSLIG Technical Notes, 7, AUSLIG, Canberra

Titov O, Tregoning P (2004) Post-seismic motion of Gilcreek Geodetic Sites following to the November, 2002 Denali Earthquake, In: Vandenberg N, Baver KD (eds) Proceedings of IVS 2004 General Meeting, NASA/CP-2004-212255, pp 496–499